Terbit *online* pada laman web jurnal : http://metal.ft.unand.ac.id

METAL: Jurnal Sistem Mekanik dan Termal

| ISSN (Print) 2598-1137 | ISSN (Online) 2597-4483 |

Research article

Synthesis and Characterization of Hydroxyapatite Derived from Pleco Fish (Hypostomus Plecostomus) Bone Waste via Calcination and Ball Milling for Biomedical Applications

Nurfitri Rahmi Sari[1], *Andika Thoriq*[1], *Gunawarman*[1], *Is Prima Nanda*[1], *Ade Indra*[2], *Yuli Yetri*[3], *Riza Verdian*[1]

[1]*Faculty of Engineering, Department of Mechanical Engineering, Universitas Andalas, Limau manis, 25166, Padang, Indonesia*
[2]*Faculty of Engineering, Department of Mechanical Engineering, Institut Teknologi Padang, KP. Olo, 25143, Padang, Indonesia*
[3]*Department of Mechanical Engineering, Politeknik Negeri Padang, Limau manis, 25166, Padang, Indonesia*

ARTICLE INFORMATION

Article History:
Received : 1 April 2025
Revised : 27 April 2025
Accepted : 30 April 2025

KEYWORDS

Hydroxyapatite
Pleco fish
Calcination
Ball milling
Biomedical applications

CORRESPONDENCE

E-mail: gunawarman@eng.unand.ac.id

A B S T R A C T

Hydroxyapatite (HA), a calcium phosphate-based bioceramic, is widely recognized for its excellent biocompatibility and bioactivity, making it suitable for biomedical applications. This study aims to synthesize HA from waste bones of the pleco fish (Hypostomus plecostomus), a natural source of calcium and phosphate that is underutilized in West Sumatera. The synthesis was conducted through calcination at 900 °C followed by mechanical refinement using ball milling for 3, 6, and 9 hours. X-ray diffraction (XRD) analysis confirmed the formation of crystalline HA with dominant peaks at 25.9°; 31.8°; and 32.9°, which remained stable across all milling durations. Scanning electron microscopy (SEM) revealed morphological transformation from coarse aggregates to more rounded particles, with increased agglomeration at longer milling times. Particle size analysis showed the smallest average particle size (3.03 µm) after 3 hours of milling, which increased to 4.29 µm at 6 hours due to agglomeration, and slightly decreased to 3.91 µm after 9 hours. Fourier transform infrared spectroscopy (FTIR) detected characteristic OH^-, CO_3^{2-}, and PO_4^{3-} functional groups. Elemental composition analysis indicated a Ca/P atomic ratio approaching the stoichiometric value of 1.67, with the highest Ca and P content achieved after 6 hours of milling. These results suggest that pleco fish bones can be effectively converted into biogenic HA with promising potential as an eco-friendly and cost-efficient biomaterial for biomedical applications.

1. INTRODUCTION

There Hydroxyapatite (HA), the main organic component of bone and teeth, has been extensively applied as a biomaterial due to its excellent biocompatibility and bioactivity. HA can be synthesized from various organic sources, such as fish bones [1]–[6], bovine bone [7]–[9], pig bone [10], [11], seashells [12], [13], eggshells [14]–[18], snail shell [19]. Several synthesis methods have been employed to produce HA, including calcination [4], [20]–[23], hydrothermal [24], [25], sol-gel [26]. The stoichiometric Ca/P ratio of HA is 1.67, which resembles the Ca/P found in natural bone and teeth [27]. HA derived from organic sources contains trace elements such as Zn, Mg, Al, Sr, K, and Na, which are known to support and enhance bone regeneration [28].

The pleco fish, a freshwater species widely distributed across Indonesia, is generally underutilized, particularly in West Sumatera, where it is often discarded as waste. This presents both an

https://doi.org/ 10.25077/metal.9.1.14-20.2025

environmental challenge and an opportunity for resource recovery. The utilization of the pleco fish bones as a raw material for HA synthesis serves as a sustainable strategy to reduce organic waste and lower dependency on imported HA. Fish bones are rich calcium and phosphate, making them a promising natural source for HA production. Furthermore, the use of such organic waste offers a cost-effective alternative to conventional synthetic routes.

Therefore, this study aims to synthesize HA from pleco fish bones through a calcination method, followed by mechanical refinement using a ball milling process. The effect of different milling durations on the particle size of resulting HA powder is evaluated to obtain optimal characteristics for potential biomedical applications.

2. MATERIALS AND METHODS

2.1. Materials

The pleco fish were collected from a river located in Padang, West Sumatera, Indonesia. Analytical grade aceton (98%), ethanol, and distilled water. Zirconia balls with a diameter of 5 mm were used as the milling media.

2.2. Methods

The Pleco fish was boiled for 90 minutes to separate the bones from the soft tissues. The extracted bones were subsequently immersed in aceton for 24 hours to eliminate residual organic matter. The bones were thoroughly washed and dried in the sunlight. The bones were ground using a blender to obtain a coarse powder. The powder was calcined in an IFU Muffle Furnace at 900 ºC with a heating rate of 10 ºC/min and a holding time of 3 hours. The calcined bone powder was allowed to cool to room temperature within the furnace. The calcined bone was manually ground to a particle size of 63 µm using a mortar and pestle. The powder was further milled using a Planetary Mill Pulverisette 6 Classic Line with a 250 mL jar and 5 mm zirconia balls. The ball-to-powder weight ratio was 10:1, and milling was performed at a rotational speed of 150 rpm with time variations of 3, 6, and 9 hours.

The phases formed during the calcination process were characterized using X-ray diffraction (XRD, PANalytical, Type PW3040/60, Netherlands). The X-ray diffractometer operated with a Cu Kα anode (λ=1,54060 Å, 2θ= 10-100º), 40 kV, and 30 mA. Fourier Transform Infrared Spectroscopy (FTIR) was employed to identify the functional groups present in the hydroxyapatite (HA) powder. Scanning Electron Microscopy (SEM) was utilized to observe the particle morphology of HA, and a Particle Size Analyzer (PSA) was used to determine the particle size of HA.

3. RESULTS AND DISCUSSION

3.1. X-ray Diffraction Result

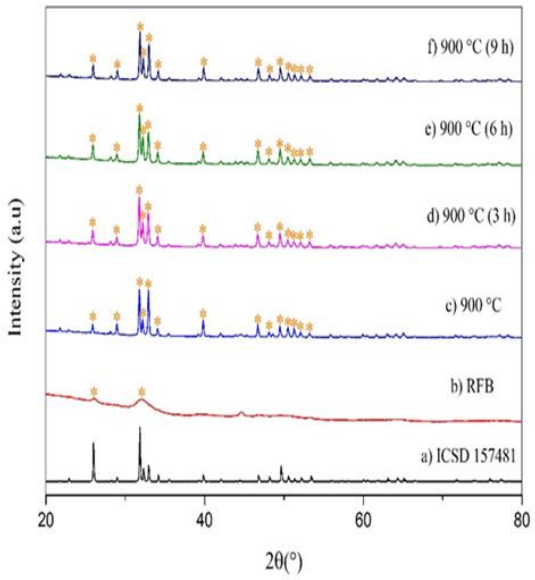

Figure 1. XRD characterization of HA powder a) Standard HA ICSD 157481, b) RFB, c) 900 ºC, d) 900 ºC (3h), e) 900 ºC (6h), f) 900 ºC (9h)

Fig.1. X-ray diffraction (XRD) patterns illustrate the phase differences among raw fish bone (RFB), fish bone powder after calcination at 900 ºC, and ball milling for 3, 6, and 9 hours. Based on the standard for HA, the main diffraction peaks are located at 25.9º; 31.8º; and 32.9º. Before the calcination process, raw fish bone (RFB) exhibited low-intensity peaks, indicating the presence of an amorphous phase, particularly at 25.9º and 31.9º. After calcination at 900 ºC, the intensity of the HA peaks increased significantly, suggesting the decomposition of organic components. The main diffraction peaks of fish bone powder calcined at 900 ºC before ball milling were observed at 25.8º; 31.7º; and 32.8º. The main diffraction peaks of fish bone powder after ball milling were consistently

observed at 25.9º; 31.8º; and 32.9º. These peaks remained stable regardless of the milling duration (3, 6, and 9 hours), indicating that the ball mill process did not significantly affect the HA phase

3.2. Surface Morphology of HA Powder

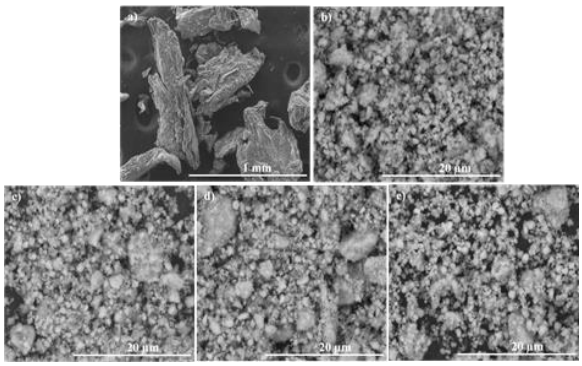

Figure 2. SEM of HA powder at different processing stages: (a) Raw Fish Bone (RFB) at 100× magnification; (b) Calcined at 900 °C at 500×; (c) Ball milled for 3 hours at 500×; (d) Ball milled for 6 hours at 500×; (e) Ball milled for 9 hours at 500×

Fig.2. SEM images showing the morphological evolution of hydroxyapatite (HA) powder derived from pleco fish bone. (a) Raw fish bone (RFB) before calcination, showing coarse agglomerates; (b) After calcination at 900 °C, the powder begins to separate but remains rough; (c) After 3 hours of ball milling, the particles are more spherical with relatively uniform size distribution; (d) After 6 hours of ball milling, partial spherification and agglomeration are observed; (e) After 9 hours of ball milling, the particles appear rounded, but agglomeration increases due to extended milling time.

3.3. Particle Size of HA Powder

Fig.3. presents the particle size and size distribution of hydroxyapatite (HA) powder analyzed using a Particle Size Analyzer (PSA). The calcination of Pleco fish bone powder at 900 °C resulted in an average particle size of 3.7216 µm. The d10 value of 2.0627 µm indicates the emergence of fine particles during the heating process.

After ball milling for 3 hours, the particle size was reduced to 3.0304 µm. Interestingly, samples subjected to 6 and 9 hours of ball milling exhibited particle sizes of 4.293 µm and 3.913 µm, respectively. The d10 value for the 3-hour milled sample was 0.6233 µm, indicating that 10% of the particles were below this size—evidence of very fine particles. The d50 value of 6.3861 µm shows that 50% of the particles were smaller than this size, representing the most common particle size in the sample. Meanwhile, the relatively high d90 and d99 values of 9.1026 µm and 9.9081 µm, respectively, suggest the presence of larger particles in the distribution.

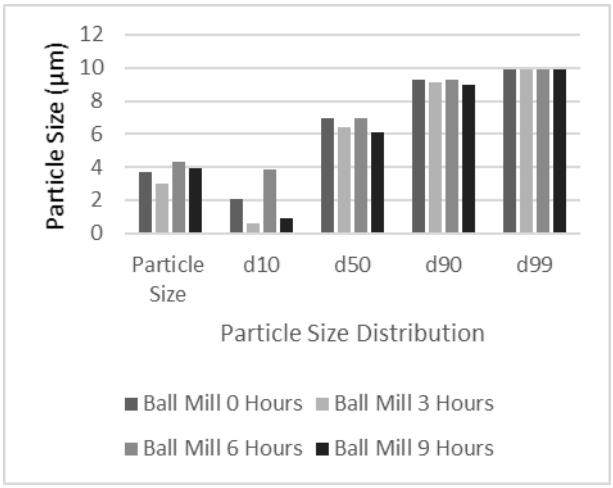

Figure 3. Particle size and distribution of HA powder.

During the 6-hour ball milling process, the d10 value increased to 3.8175 µm, indicating that the smallest particles in this sample were larger than those obtained after 3 hours of ball milling. This increase is attributed to the agglomeration of fine particles. The d50 value was 6.9606 µm, showing that 50% of the particles had sizes below this value, which is also larger compared to the 3-hour milling sample. The relatively high d90 and d99 values—9.2857 µm and 9.9272 µm, respectively—further indicate the presence of larger particles in the sample, also caused by agglomeration. Extended ball milling for 6 hours likely led to the re-agglomeration of previously formed fine particles due to continuous mechanical energy input. This agglomeration caused smaller particles to adhere and merge into larger aggregates, resulting in an overall increase in particle size.

 https://doi.org/ 10.25077/metal.9.1.14-20.2025

After 9 hours of ball milling, the d10 value was relatively small at 0.9293 µm, indicating that 10% of the particles were smaller than this size, suggesting the presence of very fine particles. The d50 value was 6.0813 µm, showing that 50% of the particles had sizes below this value, which is smaller than that observed in the 6-hour ball milling process. Although the d90 and d99 values remained relatively high, indicating the presence of larger particles in the sample, these values were lower compared to those obtained after 6 hours of milling. This suggests that prolonged milling reduced the extent of agglomeration observed at 6 hours and promoted further fragmentation of larger particles. Excessive ball milling time can lead to particle agglomeration, which reduces the effectiveness of particle size reduction and results in an increase in the average particle size of the powder [29].

3.4. FTIR Result

Fig.4 presents the functional group characterization of fish bone powder using Fourier Transform Infrared Spectroscopy (FTIR). In the raw fish bone (RFB) sample, absorption peaks were observed around 2915 cm-1 and 1625 cm-1, indicating the presence of organic compounds such as fats and proteins before the calcination process. After calcination at 900 ºC, these peaks disappeared, suggesting the decomposition of organic matter during the calcination. Additionally, the hydroxyl (OH-) group was identified at approximately 3560 cm-1[1].

The OH- group exhibited a weak absorption band at 3742 cm-1 in the RFB sample. After the calcination and ball milling process, this band showed a slight shift but remained detectable within the range 3725-3742 cm-1. The carbonate (CO32-) was identified in the range of 1400-1500 cm-1. The presence of absorption bands at approximately 1451 cm-1 and 1437 cm-1 indicates the incorporation of CO32-, likely due to the organic origin of the HA. The phosphate (PO43-) group exhibited characteristic absorption bands around 1012-1017 cm-1, 1008 cm-1, 556 cm-1, and 560 cm-1. The band in the 1005-1008 cm-1 range represents the main PO43- in the HA [30].

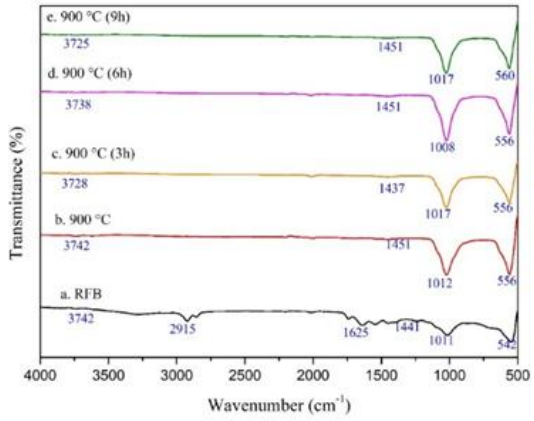

Figure 4. Powder characterization a) RFB, b) 900 ºC, c) 900 ºC (3h), d) 900 ºC (6h), e) 900 ºC (9h)

3.5. Composition of HA Powder

Table 1. presents the elemental composition of HA powder at different processing stages. The calcium (Ca) content increased significantly from 16.87% in raw fish bone (RFB) to 19.31% after calcination at 900 °C, indicating effective removal of organic contaminants and enhancement of Ca purity. Ball milling for 3 hours obtained 19.40% calcium. Further ball milling for 6 hours resulted in the highest Ca content (23.50%), suggesting improved purification. However, a decrease to 17.99% after 9 hours of milling may be attributed to structural degradation or contamination during prolonged milling.

The phosphate (P) content also increased from 4.16% (RFB) to 10.01% post-calcination. Ball milling for 3 hours obtained 10.57% phosphate. A further increase to 12.36% was observed after 6 hours of ball milling, indicating better homogenization and purification. A slight decline to 9.50% after 9 hours of milling could result from phosphate degradation due to extended processing time. Oxygen (O) content rose from 78.97% (RFB) to 70.68% after calcination, as organic matter and water were removed, and oxygen remained bound in oxide form. Ball milling for 3 hours obtained 70.03% oxigen. A reduction to 64.14% after 6 hours of milling may reflect improved decontamination, while a subsequent increase to 72.50% after 9 hours could be due to oxidation or environmental contamination during prolonged milling. The Ca/P

ratios for RFB, 900 °C, 900 °C (3 h ball milling), 900 °C (6 h ball milling), and 900 °C (9 h ball milling) were 4.05; 1.92; 1.83; 1.90; and 1.89, respectively. Several studies utilizing fish bones as a natural source of hydroxyapatite have reported varying Ca/P ratios depending on the species. Black tilapia fish bones calcined at 900 °C resulted in a Ca/P ratio of 1.56 [28], whereas C. chanos bones treated under the same calcination temperature yielded a lower Ca/P ratio of 1.74 [31].

Table 1. Composition of HA powder.

Sample	Element	Weight %	Atomic %
RFB	Ca	11.85	16.87
	P	2.26	4.16
	O	22.17	78.97
900°C	Ca	32.13	19.31
	P	12.87	10.01
	O	47.01	70.68
Ball Mill 3 hours	Ca	29.86	19.40
	P	12.57	10.57
	O	43.03	70.03
Ball Mill 6 hours	Ca	36.88	23.50
	P	15.00	12.36
	O	40.17	64.14
Ball Mill 9 hours	Ca	28.53	17.99
	P	11.64	9.50
	O	45.94	72.50

4. CONCLUSION

This study successfully synthesized hydroxyapatite (HA) from pleco fish bone waste through calcination at 900 °C followed by ball milling. The calcination process effectively eliminated organic content and promoted the formation of crystalline HA. XRD analysis confirmed that the HA phase remained stable during the mechanical milling process up to 9 hours. SEM and particle size analysis revealed that 3 hours of milling produced the finest and most uniform particles, while longer durations resulted in agglomeration. FTIR spectra identified functional groups typical of HA, and elemental analysis showed that the Ca/P ratio closely approached the ideal stoichiometry, with the highest purity observed after 6 hours of milling. Overall, pleco fish bones present a promising alternative source for producing biogenic HA, offering sustainable waste management and potential for low-cost biomedical material development.

Acknowledgement

This research was funded by Universitas Andalas under Hibah Penelitian Skripsi Sarjana (PSS) with contract no.162/UN16.19/PT.01.03/PSS/2024. The authors would like to express their gratitude to the Metallurgy Laboratory of Universitas Andalas for supporting this research

REFERENCES

[1] K. M. I. Ismail, C. N. A. Jaafar, I. Zainol, and M. Z. M. . Yusoff, “Preparation and Characterization of Hydroxyapatite from Black Tilapia Fish Scales using Spray-drying Method,” Malaysian J. Microsc., vol. 15, pp. 155–163, 2019.

[2] M. Bahraminasab, N. Doostmohammadi, and A. Alizadeh, “Low-cost synthesis of nano-hydroxyapatite from carp bone waste: Effect of calcination time and temperature,” Int. J. Appl. Ceram. Technol., vol. 18, no. 3, pp. 573–582, May 2021, doi: 10.1111/ijac.13678.

[3] D. A. Challoob, A. T. Saleh, A. Z. Alshemary, Y. Muhammed, and I. S. Cardakli, “Characterisation and in vitro bioactivity of hydroxyapatite extracted from carp fish bones for biomedical applications,” Ceram. - Silikaty, vol. 67, no. 1, pp. 81–86, 2023, doi: 10.13168/cs.2023.0005.

[4] L. Anggresani, Y. N. Sari, and Rahmadevi, “Hydroxyapatite (HAp) From Tenggiri Fish Bones As Abrasive Material In Toothpaste Formula,” J. Kim. Val., vol. 7, no. 1, pp. 1–9, May 2021, doi: 10.15408/jkv.v7i1.19165.

[5] N. R. Sari, R. Verdian, A. Indra, I. P. Nanda, R. A. Fitria, and Gunawarman, “Enhancing the Potential of Pleco Fish Bones (Hypostomus Plecostomus) With Gradual Heating and Ball Milling Methods for Biomedical Applications,” Ceram. - Silikaty, vol. 69, no. 1, pp. 2–XX, 2025, doi: 10.13168/cs.2024.0072.

[6] N. R. Sari, R. Verdian, A. Indra, I. P. Nanda, and Gunawarman, “Evaluating the Impact of Calcination Temperature on the Production of Hydroxyapatite from Fish Bones: Literature Review,” AIP Conf. Proc., vol. 3223, no. 1, 2025, doi: 10.1063/5.0243402.

[7] Gunawarman, I. H. Mulyadi, Z. Arif, N. F. Nuswantoro, J. Affi, and M. Niinomi, “Effect of Particle Size on Adhesion Strength of Bovine Hydroxyapatite Layer on Ti-12Cr

Coated by using Electrophoretic Deposition (EPD) Method," IOP Conf. Ser. Mater. Sci. Eng., vol. 1041, no. 1, p. 012054, Jan. 2021, doi: 10.1088/1757-899x/1041/1/012054.

[8] Z. Catalgol, "Sintering effect on borosilicate glass-bovine hydroxyapatite composites," J. Aust. Ceram. Soc., vol. 55, no. 4, pp. 1075–1079, Dec. 2019, doi: 10.1007/s41779-019-00320-y.

[9] Y. Yetri, Ikhsan, A. Indra, J. Affi, and Gunawarman, "Extraction of hydroxyapatite from bovine bones: The manufacturing development and its behavior properties towards acrylic resin/hydroxyapatite/alumina composites," Mater. Chem. Phys., vol. 319, no. April, p. 129244, 2024, doi: 10.1016/j.matchemphys.2024.129244.

[10] M. Rabiei, A. Palevicius, A. Monshi, S. Nasiri, A. Vilkauskas, and G. Janusas, "Comparing methods for calculating nano crystal size of natural hydroxyapatite using X-ray diffraction," Nanomaterials, vol. 10, no. 9, pp. 1–21, Sep. 2020, doi: 10.3390/nano10091627.

[11] E. A. Ofudje, A. Rajendran, A. I. Adeogun, M. A. Idowu, S. O. Kareem, and D. K. Pattanayak, "Synthesis of organic derived hydroxyapatite scaffold from pig bone waste for tissue engineering applications," Adv. Powder Technol., vol. 29, no. 1, pp. 1–8, Jan. 2018, doi: 10.1016/j.apt.2017.09.008.

[12] K. M. Balabadra, S. Panneer Selvam, R. Ramadoss, and S. Sundar, "Hydroxyapatite synthesis and characterization from marine sources: A comparative study," J. Oral Biol. Craniofacial Res., vol. 14, no. 6, pp. 706–711, Nov. 2024, doi: 10.1016/j.jobcr.2024.09.009.

[13] R. Mustaffa, M. R. Mohd Yusof, and Y. Abdullah, "A Novelty of Synthetic Hydroxyapatite from Cockle Shell and Characterization," Adv. Mater. Res., vol. 1087, pp. 429–433, Feb. 2015, doi: 10.4028/www.scientific.net/amr.1087.429.

[14] M. Akram, R. Ahmed, I. Shakir, W. A. W. Ibrahim, and R. Hussain, "Extracting hydroxyapatite and its precursors from natural resources," Journal of Materials Science, vol. 49, no. 4. pp. 1461–1475, Feb. 2014. doi: 10.1007/s10853-013-7864-x.

[15] M. U. Jahangir et al., "Comparative analysis and antibacterial properties of thermally sintered apatites with varied processing conditions," J. Am. Ceram. Soc., vol. 104, no. 2, pp. 1023–1039, Feb. 2021, doi: 10.1111/jace.17525.

[16] D. Muthu, G. S. Kumar, V. S. Kattimani, V. Viswabaskaran, and E. K. Girija, "Optimization of a lab scale and pilot scale conversion of eggshell biowaste into hydroxyapatite using microwave reactor," Ceram. Int., vol. 46, no. 16, pp. 25024–25034, Nov. 2020, doi: 10.1016/j.ceramint.2020.06.288.

[17] G. S. Kumar and E. K. Girija, "Flower-like hydroxyapatite nanostructure obtained from eggshell: A candidate for biomedical applications," Ceram. Int., vol. 39, no. 7, pp. 8293–8299, Sep. 2013, doi: 10.1016/j.ceramint.2013.03.099.

[18] S. M. Mousavi et al., "Antibacterial and cytotoxic efficacy of Nano- Hydroxyapatite Synthesized from Eggshell and Sheep bones bio Waste." Oct. 27, 2022. doi: 10.21203/rs.3.rs-2195140/v1.

[19] H. Fajri, J. Affi, and R. Syahemi Putra, "Synthesize and Characterization of Hydroxyapatite from Freshwater Snail Shell Sulcospira Sp. Proceed by Combination of Ball Milling and Heat Treatment," J. Ocean. Mech. Aerospace-Science Eng., vol. 37, pp. 9–14, 2016.

[20] J. K. Odusote, Y. Danyuo, A. D. Baruwa, and A. A. Azeez, "Synthesis and characterization of hydroxyapatite from bovine bone for production of dental implants," J. Appl. Biomater. Funct. Mater., vol. 17, no. 2, Apr. 2019, doi: 10.1177/2280800019836829.

[21] M. R. Hasan, N. S. M. Yasin, M. S. M. Ghazali, and N. F. Mohtar, "Proximate and morphological characteristics of nano hydroxyapatite (nano HAP) extracted from fish bone," J. Sustain. Sci. Manag., vol. 15, no. 8, pp. 9–21, 2020, doi: 10.46754/JSSM.2020.12.002.

[22] M. Z. Jaffri, Z. M. M. Ismail, S. K. Dermawan, and H. Z. Abdullah, "Sample Preparation of the Natural Source Hydroxyapatite (HAp) derived from Black Tilapia Fish Scales," in Journal of Physics: Conference Series, Jan. 2022, vol. 2169, no. 1. doi: 10.1088/1742-6596/2169/1/012033.

[23] A. Esmaeilkhanian, F. Sharifianjazi, A. Abouchenari, A. Rouhani, N. Parvin, and M. Irani, "Synthesis and Characterization of Natural Nano-hydroxyapatite Derived from Turkey Femur-Bone Waste," Appl. Biochem. Biotechnol., vol. 189, no. 3, pp. 919–932, Nov. 2019, doi: 10.1007/s12010-019-03046-6.

[24] A. Fadli, S. R. Yenti, R. Rasyidin, and M. Sari, "The effect of time and number of balls on shaker milling process in hydroxyapatite powder synthesis," in IOP Conference Series: Materials Science and Engineering, 2019, vol. 532, no. 1. doi: 10.1088/1757-899X/532/1/012012.

[25] A. Shavandi, A. E. D. A. Bekhit, A. Ali, and Z. Sun, "Synthesis of nano-hydroxyapatite (nHA) from waste mussel shells using a rapid microwave method," Mater. Chem. Phys., vol. 149, pp. 607–616, Jan. 2015, doi: 10.1016/j.matchemphys.2014.11.016.

[26] R. Adamski and D. Siuta, "Mechanical, structural, and biological properties of chitosan/hydroxyapatite/silica composites for bone tissue engineering," Molecules, vol. 26, no. 7, 2021, doi: 10.3390/molecules26071976.

[27] M. F. Alif, S. Arief, Y. Yusuf, Y. Yunita, J. Ramadhani, and S. Triandini, "Synthesis of hydroxyapatite from Faunus ater shell biowaste," Next Mater., vol. 3, p. 100157, Apr. 2024, doi: 10.1016/j.nxmate.2024.100157.

[28] S. K. Dermawan, Z. M. M. Ismail, M. Z. Jaffri, and H. Z. Abdullah, "Effect of the Calcination Temperature on the Properties of Hydroxyapatite from Black Tilapia Fish Bone," in Journal of Physics: Conference Series, Jan. 2022, vol. 2169, no. 1. doi: 10.1088/1742-6596/2169/1/012034.

[29] Z. Kong, Z. Wang, B. Chen, Y. Li, and R. Li, "Effect of Ball Milling Time on the Microstructure and Properties," Materials (Basel)., vol. 15, no. 5763, 2023.

[30] M. U. R. Rehman, A. Qureshi, and M. M. Baloch, "Extraction of Hydroxyapatite from Caprine Bones and its Anti-Bacterial Study," Mehran Univ. Res. J. Eng. Technol., vol. 40, no. 4, pp. 867–873, Oct. 2021, doi: 10.22581/muet1982.2104.16.

[31] H. A. Permatasari, R. Wati, R. M. Anggraini, A. Almukarramah, and Y. Yusuf, "Hydroxyapatite extracted from fish bone wastes by heat treatment," in Key Engineering Materials, 2020, vol. 840 KEM, pp. 318–323. doi: 10.4028/www.scientific.net/kem.840.318.